Available online at www.sciencedirect.com
SCIENCE DIRECT
Polymer 46 (2005) 719–724
polymer
www.elsevier.com/locate/polymer

Influence of fillers on free volume and gas barrier properties in styrene-butadiene rubber studied by positrons

Z.F. Wang[a], B. Wang[a,*], N. Qi[a], H.F. Zhang[b], L.Q. Zhang[b]

[a]*Department of Physics, Wuhan University, Wuhan 430072, Peoples Republic of China*
[b]*College of Material Science and Engineering, Beijing University of Chemical Technology, Beijing 100029, Peoples Republic of China*

Received 29 August 2004; received in revised form 18 November 2004; accepted 1 December 2004
Available online 18 December 2004

Abstract

The measurements of free-volume hole property by positron annihilation lifetime spectroscopy (PALS) have been carried out for polymer–clay nanocomposite materials that consist of styrene–butadiene rubber (SBR) and layered silicate clay of rectorite and conventional composite materials N326 (carbon black) /SBR. The PALS and differential scanning calorimeter (DSC) results show layered rectorite has a stronger effect on restraining polymer chain mobility which results in the decrease of fraction free volume and gas permeation than carbon black. The dispersion of nanoscale rectorite clay in SBR largely enhances gas barrier property in contrast to results obtained in N326/SBR system. Experimental results reveal that gas permeability in rectorite/SBR nanocomposite is mainly influenced by fractional free volume and tortuous diffusional path effects attributed to the clay plateletlike morphology.

Keywords: Positron annihilation; Nanocomposite; Fractional free volume

1. Introduction

Organic–inorganic polymer nanocomposites have attracted wide interest, because the addition of nanoparticles to polymers can enhance conductivity, mechanical toughness, optical activity and gas barrier [1–4]. A great enhancement in the gas barrier properties compared to conventional phase separated composites has been reported in polyimide, polyaniline and poly(methyl methacrylate) due to nanoscopic dispersion of the layered silicate in a polymer matrix [4–6]. The soft rubbery materials which have a characteristic elastic behavior have been used for many important engineering products containing highly compressed air, such as tires inner-tubes, air springs and cure bladders, etc [7]. Recently, a versatile and environmentally benign approach has been developed for the preparation of nanocomposites of elastomeric matrix based on rubber latex [8–9]. In the present article, we used a styrene–butadiene rubber (SBR) latex and the layered silicates of rectorite to prepare the clay/SBR nanocompoites. Rectorite is an interstratified layered silicate mineral consisting of a regular (1:1) stacking of mica-like layers and montmorillonite-like layers [10], which is mainly used as catalysts and almost has not been investigated in the application of polymer-layered silicate nanocomposites. In rectorite, only the montmorillonite-like layers can exchange charge-compensating mono- and divalent cations with large polyoxocations of Al (or Zr) to form a microspace separated by two silicate layers that impart to the expanded clay structure the more stability and strong.

Free-volume theories of gas permeability in polymers based on the original work of Cohen and Turnbull [11] are widely applied to obtain a general polymer structure-property relationship [12–14]. Positron annihilation lifetime spectroscopy (PALS) is an effective method to detect the free volume space on the basis of the fact that the positronium (Ps) atoms are formed and localized in the nanometer-scale holes in various materials. The size and shape of holes available in a polymer control the rate of gas diffusion and its permeation properties. Free volume,

* Corresponding author. Tel.: +86 27 6875 2370; fax: +86 27 8765 4569.
E-mail address: bwang@positron.whu.edu.cn (B. Wang).

0032-3861/$ - see front matter © 2004 Elsevier Ltd. All rights reserved.
doi:10.1016/j.polymer.2004.12.002

whether static voids created by inefficient chain packing or transient gaps generated by thermally induced chain segment rearrangement, presents diffusing molecules with a low-resistance avenue for transport. A simplified free-volume hole theory gives a relationship between the diffusion coefficient, D, and the fractional free volume, f_V, as [15]:

$$D = A \exp(-B/f_V) \tag{1}$$

where A is related to the size and shape of the diffusion molecule, B is related to the minimal hole size of polymer matrix required for a diffusional jump or hopping to occur and f_V is the fractional free volume which can reflect any change in amorphous regions where gas molecule can permeate.

In this study, we investigated the effects of layered silicate and carbon black (CB) fillers on the free volume properties in styrene–butadiene rubber (SBR) composites using PALS. Free volume theory was applied to investigate the effect of the free volume and morphology on gas barrier.

2. Experimental

2.1. Sample preparation

First, natural rectorite was dispersed in water with strong stirring for 5 h and an aqueous suspension of silicate was achieved. To purify natural rectorite, the aqueous suspension was kept for 24 h at room temperature and the deposition was rejected. Then the interfacial agent and the SBR latex were added into the aqueous suspension and stirred for 20 min. Finally, the mixture was coagulated by cation-type coagulating agent, washed with water several times until its pH was about 7, and then dried at 70 °C for 24 h. We obtained rectorite/SBR nanocomposites and other composites prepared by blending SBR and N326 (a type of carbon black) named N326/SBR at different amount of the filler content. The samples were prepared in College of Material Science and Engineering of Beijing University of Chemical Technology.

2.2. Sample characterization

All PAL spectra were recorded at room temperature with an Ortec 'fast-fast' lifetime spectrometer. The time resolution was 270 ps (fwhm). We used a ^{22}Na with 20 μCi as radioactive positron source and put the source between two pieces of same samples like sandwich. Each spectrum contained, approximately 1×10^6 and 4×10^6 counts for finite-term lifetime analysis using the PATFIT program [16] and continuous-lifetime analysis using the MELT program [17], respectively. The measured lifetime spectra were resolved into three lifetime components for finite-term lifetime analysis. We got the best χ^2 and most reasonable standard deviations. The shortest lifetime and the intermediate lifetime are attributed to the self-annihilation of *para*-positronium (*p*-Ps) and the free positron annihilation, respectively. The longest lifetime is due to *ortho*-positronium (*o*-Ps) pick-off annihilation in free-volume holes of amorphous region [18].

Using the following semiempirical equation and *o*-Ps lifetime, we obtained the average free-volume hole assumed spherical radius [19–21]:

$$\tau_3 = \frac{1}{\lambda_3} = \frac{1}{2}\left[1 - \frac{R}{R_0} + \frac{1}{2\pi}\sin\left(\frac{2\pi R}{R_0}\right)\right]^{-1} \tag{2}$$

where τ_3 (*o*-Ps lifetime) and R (hole radius) are expressed in ns and Å, respectively. R_o equals to $R+\Delta R$ where ΔR is the fitted empirical electron layer thickness ($=1.66$ Å). The relative fractional free volume is expressed as follows:

$$f_V = C\left(\frac{4\pi R^3}{3}\right) I_3 \tag{3}$$

where I_3 (in %) is the *o*-Ps intensity and C is a constant.

The dispersibility of the clay particles in the matrix was checked by transmission electron microscopy (TEM) using a Hitach H-800 TE microscope operated at an acceleration voltage of 200 kV. The glass transition temperature (T_g) was determined by differential scanning calorimeter (DSC) using a PerkinElmer thermal analysis apparatus at the heating rate of 10 °C/min from −150 to 100 °C. The gas permeation properties were determined for membrane samples with the diameter of 8 cm and the thickness of about 1 mm using a pressure of 0.57 Mpa and the test gas was 99.5% nitrogen. The gas permeation experiments were completed in College of Material Science and Engineering of Beijing University of Chemical Technology.

3. Results and discussions

3.1. The free-volume hole properties of SBR composites

Fig. 1 shows the TEM micrograph of rectorite/SBR nanocomposite at the filler amount of 20 per hundred parts of rubber (phr). The thick dark lines are assemblies of clay sheets and viewed edge of clay, the thickness of dispersed clay can be obtained from the width of the line. The micrograph clearly indicates that the silicate layers are dispersed into SBR at a nanometer scale (i.e. thickness of layers bundle <100 nm). No larger-scale stacks are observed. However, most of the dispersed units in the nanocomposite are not individual layer but layer bundles.

The effects of rectorite clay and carbon black filler content on *o*-Ps lifetime τ_3 and intensity I_3 for styrene–butadiene rubber composites analyzed by PATFIT program are shown in Figs. 2 and 3, respectively. Fig. 2 shows that longest lifetime τ_3 in N326/SBR is nearly the same as that in

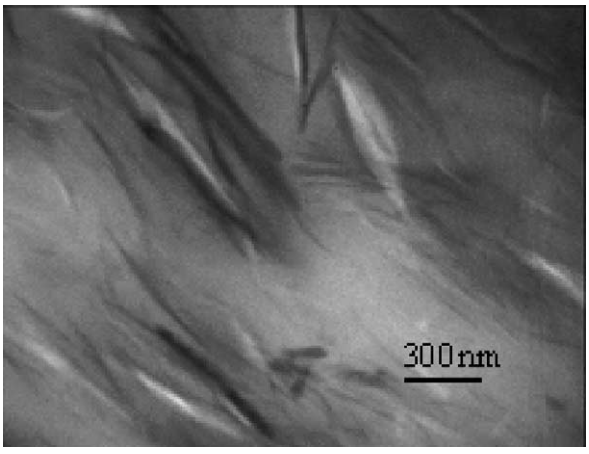

Fig. 1. TEM micrograph of rectorite/SBR.

pure SBR with the increasing volume fraction which indicates that Ps atoms are formed and annihilate only in the free-volume holes in the SBR. The similar results have been reported by Debowska et al. [22]. τ_3 in rectorite/SBR has a slight decrease attributed to stronger interaction between clay and SBR matrix resulting in the constraining effect on polymer main chains. Although the *o*-Ps lifetime changes slightly after incorporation of the filler, we observed a rapid decrease of *o*-Ps intensity I_3 with the increasing ϕ_f in Fig. 3. This observation can be explained by the following reasons. The increase of incorporation filler content brings about the decrease of volume fraction of SBR system, which results in the decrease of Ps formation probability in the SBR. On the other hand, the interaction between the matrix and the randomly distributed filler particles can restrict the main-chain segmental motion and reduce the chain mobilization in SBR matrix, which can reduce the free-volume concentration [23]. The variations of the positron intensity I_2 in the SBR composites are shown in

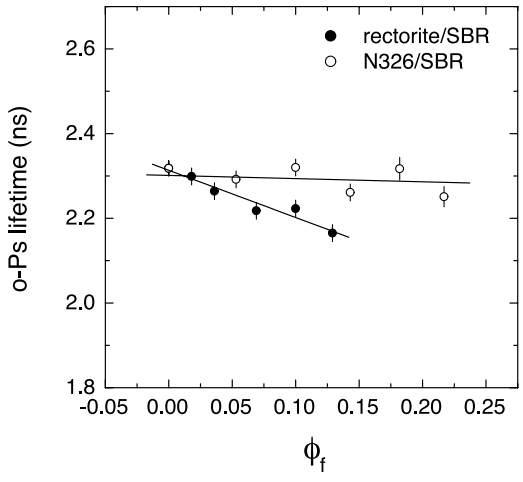

Fig. 2. Effects of the filler loading on *o*-Ps lifetime, τ_3. Filler volume fraction is estimated from $\phi_f = m_f/(m_f + m_p\rho_f/\rho_p)$, where m and ρ refer to the mass and density, respectively, of filler (f) and polymer (p) used in the SBR composites.

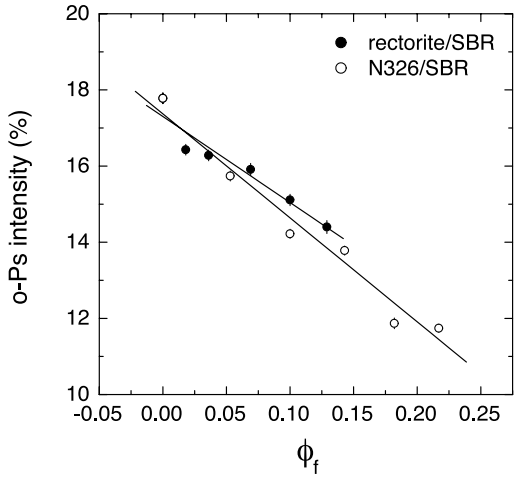

Fig. 3. Effects of the filler loading on *o*-Ps intensity, I_3.

Fig. 4. The increase of I_2 in rectorite/SBR results from the increasing fraction of positrons that annihilate in the interfacial layers between rectorite and SBR. Compared to rectorite clay, the influence of carbon black filler on I_2 of SBR is more complex. Except for the above consideration, Ps is inhibited by the CB introduced to SBR matrix taking account of the presence of radicals discovered in the CB particles [22,24]. This can explain why I_3 of N326/SBR decreases more rapidly than that of rectorite/SBR although the interaction between the filler and polymer matrix is stronger for the latter which will be discussed in detail by MELT program. Therefore *o*-Ps intensity in N326/SBR could not directly reflect the free-volume hole concentration. Table 1 shows the fractional free volume values in rectorite/SBR system decrease with the increasing ϕ_f.

In order to obtain the more detailed information of the free volume properties, the MELT program is used to determine the distributions of the free volume hole. The MELT program has been successfully applied to analysis of positron lifetime spectra in polymers [25–27]. The distributions of *o*-Ps lifetime are presented in Fig. 5 for pure SBR

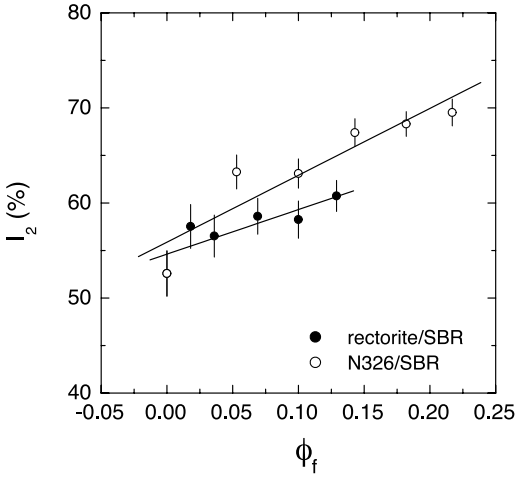

Fig. 4. Effects of the filler loading on the positron intensity, I_2.

Table 1
Relative fraction free volume, f_V, for pure SBR and rectorite/SBR

The content of rectorite filler (phr)	0	5	10	20	30	40
Fraction free volume (arb. Unit)	4.08	3.67	3.52	3.39	3.26	2.96

and SBR composites with 20 phr of filler. For the longest lived-component, the values of peaks analyzed by MELT are consistent with the results analyzed by PATFIT as shown in Table 2. From Fig. 5 and Table 2, we can observe a narrower distribution of hole size in the following order: SBR > N326/SBR > rectorite/SBR. In previous paper [12, 27], the distribution of the *o*-Ps lifetime can reflect the motion of the polymer chain and hence the difference manifest in all samples may be interpreted in terms of polymer chain packing after incorporation fillers. As shown in Fig. 1, good dispersion appears in rectorite/SBR. The large specific surface area of silicate layers will significantly inhibit polymer chain motion around nanoparticles dispersed in SBR matrix, which results in the tightness of intersegmental packing. N326/SBR has the intermediate state due to the existence of 'bound rubber' [28]. Bound rubber is trapped between or within the filler aggregates where it is no longer part of the elastically active rubber matrix. On the other hand, in rectorite/SBR, aggregation of silicate layers serves to increase the effective thickness of the dispersed unit and synchronously weaken the interaction between nanoparticles and polymer matrix, because the distance between the nanoparticles is too short and the interaction between them is too strong. Therefore the different representation in the effects of the different filler on polymer chain mobility shown in Fig. 5 can be explained. The glass transition temperature (T_g) yields the relative stiffness, i.e. the higher the T_g, the greater the polymer chain stiffness. The T_gs of these membranes determined by DSC shown in Table 2 support the results of MELT.

3.2. Effect of the free volume and morphology on gas permeability

Owing to their plateletlike morphology clay particles embedded in a polymer matrix should lower permeability and improve the barrier film properties of the polymer. Two factors can influence gas barrier property. One is the geometric factor that favors the reduction in permeability by forcing diffusing molecules to take a long way around the platelets and hence depends only on the size of clay nanoparticles. A simple tortuous two-dimensional model has been developed by Neilson to depict the effect of size on the barrier performance of polymer composites containing platelet particles [29], as can be written by the following Eq. (4):

$$P_C = P_P\left(\frac{1-\phi_f}{1+\alpha\phi_f/2}\right) \tag{4}$$

where P_c and P_p are the permeability of the composite medium and the pure polymer, respectively. ϕ_f and α are the volume fraction of filler and aspect ratio of platelets, respectively. The second factor is related to molecular level interaction of the matrix polymer with the filler, which in turn results in changes in the fractional free volume. Physically, reduced permeation in filled polymers is attributed to the increase in diffusion path length and decrease in effective cross-sectional area available for transport.

The gas permeabilities of rectorite/SBR and N326/SBR are presented in Fig. 6 in terms of P_c/P_p. At the highest filler concentration examined, the rectorite/SBR and N326/SBR

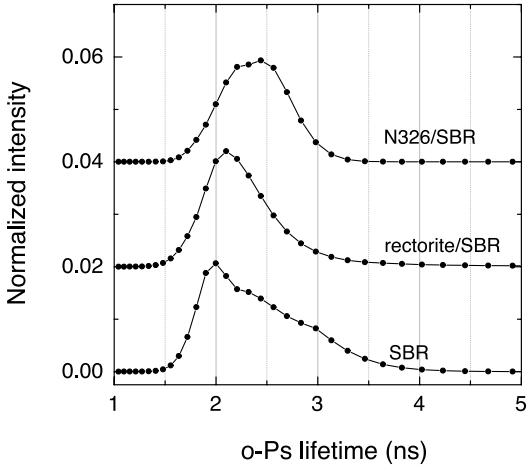

Fig. 5. *o*-Ps lifetime distribution in pure SBR, rectorite/SBR and N326/SBR at the filler content of 20 phr.

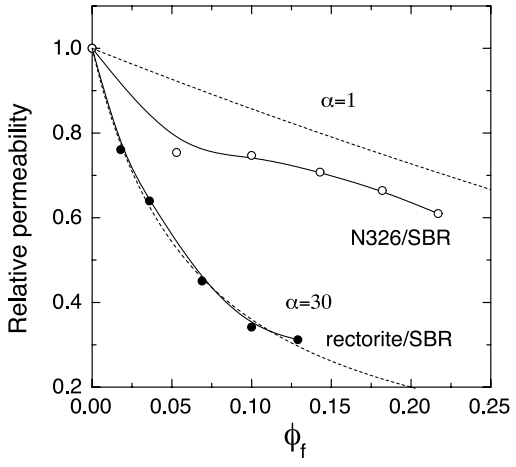

Fig. 6. Effects of the filler loading on relative permeability. The dash lines represent predictions from Eq. (4) for aspect ratio = 1 and 30, respectively.

Table 2
The *o*-Ps parameters obtained by PATFIT and MELT, and the glass transition temperature determined by DSC

Sample	τ_3(ns)	I_3(%)	FWHM(ps)	T_g(°C)
SBR	2.318±0.02	17.78±0.14		−50.02
	2.324	18.2	867.93	
Rectorite/SBR(20)	2.269±0.02	16.02±0.16		−27.21
	2.247	16.1	592.24	
N326/SBR(20)	2.321±0.02	14.22±0.12		−43.87
	2.347	14.1	666.62	

permeability are 68.8% and 39.0% lower than that of pure SBR, respectively. The reduction in gas permeability of rectorite/SBR is greater than that of N326/SBR, which is attributed to their platey morphology and high aspect ratio. The dash lines represent predictions of the Neilson equation for a particle aspect ratio of 1 and 30, respectively. The departure of our N326/SBR system from the dash line of $\alpha=1$ as for sphere morphology of carbon black particles is attributed to the decrease of fraction free volume and aggregation of CB particles. The dash line of $\alpha=30$ represents the best fit of the Neilson equation to the data of rectorite/SBR system which indicates the dispersed units of the rectorite are layer bundles supported by the TEM results after considering the original size of rectorite. Fig. 7 shows the variating diffusion coefficients in nanocomposite and N326/SBR have the similar pattern as that one depicted by permeability. The factors causing the reduction in permeability effectively affect the diffusion of the penetrant.

The solution-diffusion mechanism of membrane transport assumes that the gas permeation rate is affected by two factors: the diffusion coefficient, D, a kinetic parameter and the solubility coefficient, S, a thermodynamics parameter, which can be written as:

$$P = D \times S \tag{5}$$

As shown in Fig. 7, the reduction in diffusion are 59.5 and 25.2% for the rectorite/SBR and N326/SBR, respectively. According to Eq. (5) and the permeability and diffusion coefficients, the calculated reduction in solubility are 22.9% and 18.4% for the rectorite/SBR and N326/SBR, respectively, which indicates that the fillers of clay nanoparticles and carbon black exert a stronger effect on D than on S.

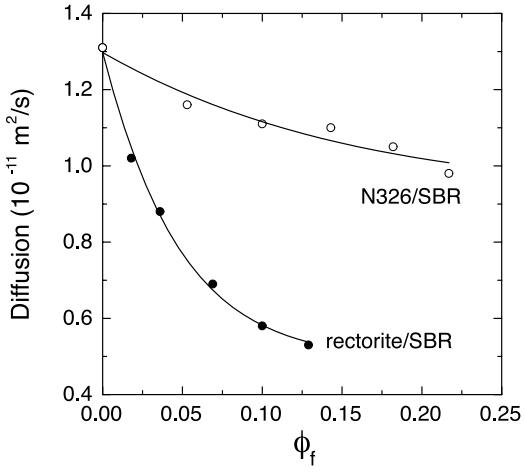

Fig. 7. Effects of the filler loading on gas diffusion.

For polymer, in addition to fractional free volume, the free volume distribution may also affect gas diffusion. A correlation between the broadening of volume distribution and gas diffusion is that a broader distribution of free-volume holes results in a larger values of gas diffusion coefficient [12]. The factors of platey morphology, lower fractional free volume and narrower distribution of free-volume result in great reduction of gas diffusion and permeability for rectorite/SBR nanocomposite compared to pure SBR. Although the effects of restricting polymer chain mobility for the clay of rectorite are stronger than for carbon black, the big difference in permeation reduction between these two composite systems may be largely owing to tortuous diffusional path effects.

For nanocomposite materials, the two factors should be considered in free volume theory: one is the tortuosity factor (τ), which is defined as the ratio of the actual distance that a penetrant must travel to the shortest distance that is would have traveled in the absence of the layered silicate, and the other is the constraining effect of the nanoparticles on the amorphous chain segments (β). After taking account of these two factors, Eq. (1) should be modified as:

$$D = \frac{A}{\tau}\exp(-B/f_V) \tag{6}$$

τ can be expressed as $1+L/2W\phi_f$ (L is the average length of the clay platelets and W is the thickness) and any change in factor β can be reflected in changes in f_V.

Fig. 8 shows the logarithm of the permeability (P) and diffusion (D) in rectorite/SBR as a function of the inverse of fractional free volume. Nonlinear relationship between permeability and diffusion and fractional free volume in rectorite/SBR clearly indicates that the reduction in permeability and diffusion is due to more than the decrease of fraction free volume. The tortuosity factor included in $\ln(A/\tau)$ seems to contribute much to variation in P and D for clay/SBR nanocomposite. The gas permeation of nanocomposite depends on not only free volume, but also the clay nanoparticles size and shape.

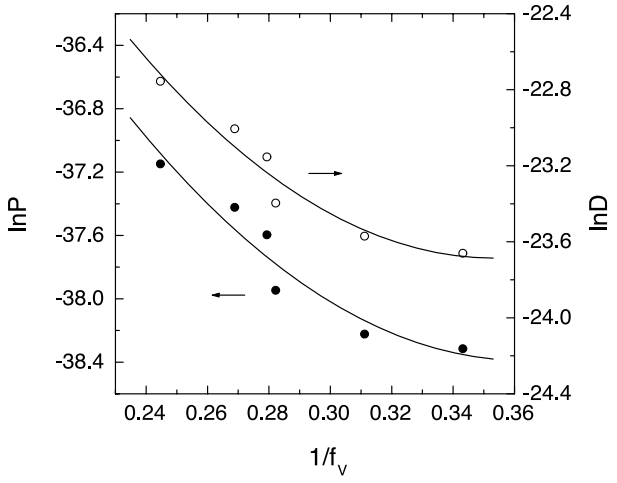

Fig. 8. Plots of the logarithm of gas permeability and diffusion as a function of the inverse fractional free volume for rectorite/SBR system.

4. Conclusion

We have presented the results of positron annihilation lifetime measurements on rectorite/SBR and N326/SBR. The free-volume hole fraction in rectorite/SBR are lower compared to pure SBR. The decrease of I_3 in N326/SBR system is due to more than the decrease of free-volume hole concentration and hence its *o*-Ps parameters can not reflect the change of the free volume. The gas barrier of rectorite/SBR exhibits a 68.8% reduction in permeability compared to Pure SBR. Incorporation of nanolayers of rectorite effectively improves gas barrier property attributed to the tortuous diffusional path and lower fractional free volume. The large difference in permeability reduction between rectorite/SBR and N326/SBR is mainly attributed to tortuous diffusional path effects. Nonlinear relationship between P and f_V in rectorite/SBR indicates that the reduction in permeability is owing to more than the decrease of fractional free volume. The gas barrier of nanocomposites is controlled by not only free volume, but also the clay nanoparticles size and shape.

Acknowledgements

This work was supported by the National Natural Science Foundation.

References

[1] Coronado E, Galan-Mascaros JR, Gomez-Garcia CJ, Laukhin V. Nature 2000;408:447.
[2] Pinnavaia TJ. Science 1983;220:365.
[3] Wang Y, Herron N. Science 1996;273:632.
[4] Lan T, Kaviratna PD, Pinnavaia TJ. Chem Mater 1994;6:573.
[5] Yeh JM, Liou SJ, Lai CY, Wu PC. Chem Mater 2001;13:1131.
[6] Yeh JM, Liou SJ, Lin CY, Cheng CY, Chang YW. Chem Mater 2002; 14:154.
[7] Nah CW, Ryu HJ, Kim WD, Choi SS. Polym Adv Technol 2002;13:649.
[8] Zhang LQ, Wang YZ, Wang YQ, Sui Y, Yu DS. J Appl Polym Sci 2000;78:1873.
[9] Wu YP, Zhang LQ, Wang YQ, Liang Y, Yu DS. J Appl Polym Sci 2001;82:2842.
[10] Grim RE. Clay minerology. New York: McGraw-Hill; 1968.
[11] Cohen MH, Turnbull D. J Chem Phys 1959;31:1164.
[12] Jean YC, Yuan JP, Liu J, Deng Q, Yang HJ. J Polym Sci Part B: Polym Phys 1995;33:2365.
[13] Wang ZF, Wang B, Yang YR, Hu CP. Eur Polym J 2003;39:2345.
[14] Eastmond GC, Daly JH, McKinnon AS, Pethrick RA. Polymer 1999; 40:3605.
[15] Fujita H. Polym J 1991;23:149.
[16] Kirkegaard P, Eldrup M, Mogensen OE, Pedersen NJ. Comput Phys Comm 1981;23:307.
[17] Shukla A, Peter M, Hoffmann L. Nucl Instr Meth A 1993;335:310.
[18] Jean YC. Microchem J 1990;42:72.
[19] Tao TS. J Chem Phys 1972;56:5499.
[20] Eldrup M, Lightbody D, Sherwood JN. Chem Phys 1981;63:51.
[21] Nakanishi H, Wang SJ, Jean YC. Positron annihilation studies of fluids. Singapore: World Science; 1988.
[22] Debowska M, Rudzinska-Girulska J, Jezierski A, Pasternak A, Pozniak R. Radiat Phys Chem 2000;58:575.
[23] Lin D, Wang SJ. J Phys Condens Matter 1992;4:3331.
[24] Ito Y. Radiation chemistry: intraspur effects and positronium formation mechanism. In: Schrader DM, Jean YC, editors. Positron and positronium chemistry. Amsterdam: Elsevier; 1998. p. 151.
[25] Wang CL, Maurer FHJ. Macromolecules 1996;29:8249.
[26] Wastlund C, Maurer FHJ. Macromolecules 1997;30:5870.
[27] Wang B, Wang ZF, Zhang M, Liu WH, Wang SJ. Macromolecules 2002;35:3993.
[28] Kohls DJ, Beaucage G. Curr Opin Solid State Mat Sci 2002;6:183.
[29] Neilson LE. J Macromol Sci (Chem) 1967;A1:929.